White Rose Research Online

eprints@whiterose.ac.uk
https://eprints.whiterose.ac.uk
Universities of Leeds, Sheffield and York

Deposited via The University of Leeds.

White Rose Research Online URL for this paper:
https://eprints.whiterose.ac.uk/id/eprint/130086/

Version: Accepted Version

Article:
Pose, S, Marcus, SE and Knox, JP (2018) Differential metabolism of pectic galactan in tomato and strawberry fruit: detection of the LM26 branched galactan epitope in ripe strawberry fruit. Physiologica Plantarum, 164 (1). pp. 95-105. ISSN: 0031-9317

https://doi.org/10.1111/ppl.12748

This article is protected by copyright. This is the peer reviewed version of the following article: Posé, S. , Marcus, S. E. and Paul Knox, J. (2018), Differential metabolism of pectic galactan in tomato and strawberry fruit: detection of the LM26 branched galactan epitope in ripe strawberry fruit. Physiologica Plantarum. doi:10.1111/ppl.12748, which has been published in final form at https://doi.org/10.1111/ppl.12748. This article may be used for non-commercial purposes in accordance with Wiley Terms and Conditions for Self-Archiving. Uploaded in accordance with the publisher's self-archiving policy.

Reuse
Items deposited in White Rose Research Online are protected by copyright, with all rights reserved unless indicated otherwise. They may be downloaded and/or printed for private study, or other acts as permitted by national copyright laws. The publisher or other rights holders may allow further reproduction and re-use of the full text version. This is indicated by the licence information on the White Rose Research Online record for the item.

Takedown
If you consider content in White Rose Research Online to be in breach of UK law, please notify us by emailing eprints@whiterose.ac.uk including the URL of the record and the reason for the withdrawal request.

UNIVERSITY OF LEEDS
University of Sheffield
UNIVERSITY of York

Accepted Article

Differential metabolism of pectic galactan in tomato and strawberry fruit: detection of the LM26 branched galactan epitope in ripe strawberry fruit

Sara Posé[†], Susan E Marcus, and J Paul Knox*

Centre for Plant Sciences, Faculty of Biological Sciences, University of Leeds, Leeds LS2 9JT, United Kingdom

Correspondence

*Corresponding author,
e-mail: J.P.Knox@leeds.ac.uk

[†]Current address: Instituto de Hortofruticultura Subtropical y Mediterránea "La Mayora" (IHSM-UMA-CSIC), Departamento de Biología Vegetal, Universidad de Málaga, 29071 Málaga, Spain

Antibody-based approaches have been used to study cell wall architecture and modifications during the ripening process of two important fleshy fruit crops: tomato and strawberry. Cell wall polymers in both unripe and ripe fruits have been sequentially solubilized and fractions analysed with sets of monoclonal antibodies focusing on the pectic polysaccharides. We demonstrate the specific detection of the LM26 branched galactan epitope, associated with rhamnogalacturonan-I, in cell walls of ripe strawberry fruit. Analytical approaches confirm that the LM26 epitope is linked to sets of rhamnogalacturonan-I and homogalacturonan molecules. The cellulase-degradation of cellulose-rich residues that releases cell wall polymers intimately linked with cellulose microfibrils has been used to explore aspects of branched galactan occurrence and galactan metabolism. In situ analyses of ripe strawberry fruits indicate that the LM26 epitope is present in all primary cell walls and also particularly abundant in vascular tissues. The significance of the occurrence of branched galactan structures in the side chains of rhamnogalacturonan-I pectins in the context of ripening strawberry fruit is discussed.

Abbreviations – AIR, Alcohol insoluble residue; CWM, Cell wall materials; DAA, Day after anthesis; EDC, Epitope detection chromatography; HG, Homogalacturonan; mAb, Monoclonal antibody; RG-I, Rhamnogalacturonan-I; RG-II, Rhamnogalacturonan-II; XG, Xyloglucan

This article has been accepted for publication and undergone full peer review but has not been through the copyediting, typesetting, pagination and proofreading process, which may lead to differences between this version and the Version of Record. Please cite this article as doi: 10.1111/ppl.12748

This article is protected by copyright. All rights reserved.

Accepted Article

Introduction

Fleshy fruits, including tomato and strawberry, are important crops worldwide and both also possess a short shelf life due to over-softening and subsequent fungal and other pest diseases. In addition to its economic relevance, tomato is also the most widely used model system for the study of the molecular mechanisms of fruit ripening (Tomato Genome Consortium 2012) and is followed by strawberry as a model system for non-climacteric fruits (Paniagua et al. 2017). Also noteworthy in this context is that while tomato fruit development goes through distinct developmental stages of cell division, cell enlargement and a final ripening phase, the equivalent stages are not so well defined in strawberry fruit (Giovannoni 2004, Perkins-Veazie 1995).

Fruit texture is a multicomponent trait dependent on tissue organization, cell morphology and cell turgor, but its main determinants are cell wall strength and adhesion between adjacent cells – factors reliant on primary cell walls and middle lamellae (Harker et al. 1997, Mercado et al. 2011, Wang et al. 2018). Plant cell walls are highly interconnected matrices of polysaccharides that need to be strong enough to generate and resist turgor pressure and at the same time modifiable in line with cell and developmental processes. Cell wall multifunctionality is underpinned by compositional and architectural heterogeneities and dynamics (Höfte and Voxeur 2017). Cell wall composition is variable but a broad view of primary cell walls of eudicotyledons indicates that they are composed of approximately 30% cellulose, 30% pectin and 30% of non-cellulosic, non-pectic polysaccharides (that is predominantly xyloglucan), and 10% of proteins and other minor components (Burton et al. 2010). In some ripe fruits pectin contents can be up to 60% of cell wall molecules (Mercado et al. 2011).

Pectins are amongst the most structurally complex polysaccharides occurring in nature with three major domains: homogalacturonan (HG) composed of linear chains of galacturonic acid (GalA) and which accounts for ~65% of pectin and is partially and variably methyl-esterified; rhamnogalacturonan-I (RG-I) being around 20 to 35% of pectin and in which a repetitive galacturonic acid and rhamnose disaccharide forms a backbone that is decorated by highly variable side chains containing arabinosyl (Ara), galactosyl (Gal) and other glycosyl residues; rhamnogalacturonan-II (RG-II) which is an extreme heteropolymer in which a HG backbone is decorated with four structurally complex side chains that are well conserved among species (Caffall and Mohnen 2009, Christiaens et al. 2016).

Extensive cell wall disassembly is considered to be the major determinant of fruit softening during the ripening process in fleshy fruits (Mercado et al. 2011, Wang et al. 2018, Posé et al. 2018). This cell wall disassembly has been widely studied for potentially extending the shelf life of soft fruits therefore reducing agronomical losses, and a firmer fruit phenotype has been produced in several cases (Jiménez-Bermúdez et al. 2002, Quesada et al. 2009, Paniagua et al. 2016, Uluisik et al. 2016, Smith et al. 2002). Specific cell wall modifications are common to almost all fruits, although to different extents depending on the fruit species (Redgwell 1997a, 1997b, Brummell 2006, Posé et al. 2018). Both tomato and strawberry fruits have a moderate pectin solubilization and a reduction in

This article is protected by copyright. All rights reserved.

Accepted Article

neutral sugars that is mainly Ara in strawberry and Gal in tomato (Seymour et al. 1990, Redgwell et al. 1997b, Brummell 2006, Paniagua et al. 2017). Although a survey in several fruits has shown a poor correlation between the loss of pectic galactosyl residues during ripening with fruit texture (Redgwell et al. 1997b) the downregulation of β-galactosidases in both tomato and strawberry transgenic lines has produced a similar 40% increment in fruit firmness over control lines (Smith et al. 2002, Paniagua et al. 2016). However, the relationships between Gal content and fruit texture remains unclear. Pectic galactan may relate to cell wall porosity influencing access of cell wall enzymes to substrates or may mediate cell wall cross-linking (Smith et al. 2002, Paniagua et al. 2016).

Many aspects and fine details of cell wall architectural modifications and cell wall dynamics during fruit ripening remain unknown. Recently, the high avidity (picogram detection range) and exquisite specificity of monoclonal antibodies (mAbs) (Ruprecht et al. 2017) have been combined with anion-exchange chromatography in an analytical procedure called epitope detection chromatography (EDC, Cornuault et al. 2014), and used to study polysaccharide populations and potential interlinkages in ripe strawberry and tomato together with aubergine and apple (Cornuault et al. 2018a). The ripe fruits of both tomato and strawberry have a similar texture (Cornuault et al. 2018b) but differ in cell wall composition and architecture. A recently described mAb LM26, binds to an epitope of branched pectic galactan – a β-1,6-galactosyl substitution of the β-1,4-galactan backbone (Torode et al. 2018). In certain organs, the LM26 epitope is detected only in phloem sieve element cell walls and in the case of grass phloem tissues it has a complementary cell patterning to the LM5 mAb 1,4-galactan epitope which is detected in companion cell walls and the patterning of these pectic galactan epitopes is correlated with a higher elasticity in LM26 rich cell wall regions (Torode et al. 2018). The LM5 mAb, first developed to study tomato fruit cell walls, is now known to bind to the non-reducing end of linear pectic 1,4-galactan (Andersen et al. 2016). Here we present data on the differential occurrence of the LM26 and LM5 pectic galactan epitopes in tomato and strawberry fruit.

Materials and methods

Monoclonal antibodies

MAbs used in this study included LM5 binding to pectic 1,4-galactan (Andersen et al. 2016), LM26 to branched pectic galactan (Torode et al. 2018), INRA-RU1 to the RG-I backbone (Ralet et al. 2010), LM6-M to pectic 1,5-arabinan (Cornuault et al. 2017), LM13 to linear 1,5-arabinan (Verhertbruggen et al. 2009a), JIM7, LM18, LM19 and LM20 to pectic HG with differential levels of esterification (Verhertbruggen et al. 2009b) and LM25 to xyloglucan (Pedersen et al. 2012).

Fruit samples and cell wall extraction and fractionation

This article is protected by copyright. All rights reserved.

Accepted Article

Tomato (*Solanum lycopersicum* L., v. Ailsa Craig) and strawberry (*Fragaria* x *ananassa* Duchesne, v. Vibrant) were grown with a 16:8 h light:dark cycle at 25°C. Tomato green-unripe and red-ripe stages were harvested at 30 days after anthesis (DAA) and 60 DAA respectively. Strawberry green-unripe and red-ripe stages were harvested at 14 DAA and 40 DAA respectively.

Cell wall extraction is described in Cornuault et al. (2018a). Briefly, fruits at the different stages were selected, peeled, sliced and lyophilized. Freeze-dried materials were milled and 0.5 g dry weight aliquots were extracted with 5 ml of phenol:water solution (4:1, w/v) to prevent cell wall degradation by endogenous enzymes (Renard et al. 2005). After 2 h at RT they were homogenized and centrifuged for 20 min at 4000 *g* and supernatants were decanted. Pellets were washed, to remove residual phenol, with 5 ml of 50 mM sodium acetate buffer pH 4, mixed and centrifuged as previously described. The supernatant was pooled with the previous one from the phenol fraction and subjected to further analysis. Pellets were sequentially washed with 70% (v/v) ethanol, 90% (v/v) ethanol, chloroform:methanol (1:1) and acetone to obtain an alcohol-insoluble residue (AIR). This AIR was de-starched by α-amylase treatment and the final cell wall materials (CWM) were precipitated in 75% (v/v) ethanol at -20°C for 24 h. Afterwards, CWM were extracted in sets of three biological replicates by a series of solvents as previously described by Santiago-Doménech et al. 2008. Briefly, 5 mg of the CWM preparations were sequentially extracted with 1 ml of: deionized water, 0.05 M *trans*-1,2-diaminocyclohexane-*N,N,N′N′*-tetraacetic acid (CDTA) in 0.05 M sodium acetate buffer, pH 6, 0.1 M Na_2CO_3 containing 0.1% (w/v) $NaBH_4$, and 4 M KOH containing 0.1% (w/v) $NaBH_4$. Before dialysis, the alkaline fractions were neutralized using acetic acid. All solubilized fractions were dialysed against distilled water using 1.5 ml Eppendorf tubes for small volume samples. Extracts were aliquoted and frozen at -20°C until use. In some cases, 5 mg of CWM were sequentially extracted with CDTA and KOH as described above but with 500 µl volumes. The insoluble residues were then washed with water (2 x 30 min) and then degraded with cellulase 5A (from *Bacillus* spp., Nzytech Lisbon, Portugal) at 1 µg ml^{-1} in 500 µl 20 mM Tris pH 8.8 for 16 h. In all cases insoluble materials were collected by centrifugation in a microfuge and supernatants retained for analysis.

ELISA, sandwich ELISA and epitope detection chromatography

Cell wall fractions (i.e. phenol, water, CDTA, Na_2CO_3 and KOH extracts) were screened with a panel of mAbs by ELISA as described (Cornuault et al. 2014). Briefly, 100 µl of a 60-fold dilution in 1X PBS of each sample was coated (in technical triplicate) onto microtitre plates overnight at 4°C. For sandwich ELISAs, microtitre plates were coated with the HG-binding CBM77 (Venditto et al. 2016) at 40 µg ml^{-1} overnight at 4°C in PBS. Plates were then blocked and then the strawberry sodium carbonate extract was diluted 60-fold in 1X PBS with 5% (w/v) skimmed milk powder for the first stage incubation prior to standard ELISA.

Cell wall extracts were further analysed by epitope detection chromatography (EDC) in anion-exchange chromatography (AEC) mode using a 1 ml HiTrap ANX FF column (GE Healthcare,

This article is protected by copyright. All rights reserved.

Accepted Article

Buckinghamshire, UK). Samples for EDC were performed using an equal 5 µl volume of the dialysed fractions, also diluted in 2.5 ml of 20 mM sodium acetate buffer pH 4.5. Samples were eluted at a flow rate of 1 ml min^{-1}, collected and analysed using ELISA as described (Cornuault et al. 2014). The salt elution gradient started with 20 mM sodium acetate buffer pH 4.5 for 13 ml, then an increasing gradient of 0–50% 0.6 M NaCl in 50 mM sodium acetate buffer pH 4.5 over 24 ml, followed by a second gradient from 50-100% 0.6 M NaCl for another 7 ml, and then 4 ml with the salt gradient at maximum (50 mM sodium acetate buffer pH 4.5, 0.6 M NaCl). In total, 48 (1 ml) fractions were collected. EDC profile data shown are the means of at least two independent chromatographic runs.

Microscopy and immunohistochemistry

Plant materials were prepared for analysis through infiltration with an ethanol series followed by LR White resin (Agar Scientific, Berkshire, England) and polymerized at 60°C as described (Lee et al. 2012). For light microscopy study of resin sections, the epoxy tissue stain that is a mixture of Toluidine Blue O and Basic Fuchsin (Electron Microscopy Sciences, Hatfield, PA) was used as metachromatic stain and applied for 5 min and thoroughly washed with water just before visualization. For indirect fluorescence of immuolabelling procedures, LM5 and LM26 hybridoma supernatants were diluted 10-fold and applied to sections using the protocol described (Lee et al. 2012). Micrographs were obtained using a Nikon Eclipse E800 epifluorescence (Tokyo, Japan) microscope and a Leica DFC450 C camera (Wetzlar, Germany).

Results

The LM26 branched galactan epitope is relatively abundant in ripe cell walls of strawberry fruit

As a starting point for the analysis, cell walls from both unripe and ripe tomato and strawberry fruits were isolated and sequential extracted/solubilized by a series of solvents. These soluble fractions were assayed with HG and RG-I mAbs to produce a heat map (Fig. 1). HG epitopes were highly detected in water, CDTA and sodium carbonate fractions of all samples. In the case of KOH fractions, low ester epitopes (LM18 and LM19) showed an opposite pattern during ripening, with a decreased signal in tomato, and an increased signal in strawberry. Similar patterns in terms of the KOH fractions was observed for some of the RG-I-directed mAbs. The INRA-RU1 epitope of the RG-I backbone was detected at a similar level in the KOH fractions of the unripe/ripe stages of both fruit. Detection of the pectic arabinan epitopes indicated lower levels in KOH fractions in ripe tomato fruits relative to unripe fruits but this was not the case for strawberry fruits where levels were similar for ripe and unripe fruits. (Fig. 1).

Interestingly, more complex differences were observed in the case of the pectic galactan epitopes. In the case of tomato, as anticipated, the LM5 epitope signal was lower in all fractions in the ripe compared to the unripe fruit whereas in strawberry the LM5 epitope levels were more similar in

This article is protected by copyright. All rights reserved.

Accepted Article

both ripe and unripe fruit cell wall fractions. The major difference across the pectic epitopes was in the detection of the LM26 epitope which was detected at only very low levels in all tomato samples and at similar low levels in unripe strawberry samples. However, the LM26 epitope was strongly detected in ripe strawberry fractions, including the KOH fraction. This indicates that the LM26 branched galactan epitope becomes strongly detectable during strawberry fruit ripening and is most abundant in polysaccharide fractions requiring alkali for solubilisation.

To further study pectic galactan during fruit ripening, the LM5/LM26 mAbs were used for epitope detection chromatography (EDC) of both fruits at both ripening stages as shown in Fig. 2. The water, sodium carbonate and KOH fractions with highest LM26 epitope levels were selected for these analyses. In Fig. 2 the vertical dotted lines on the chromatograms indicate the elution of HG epitopes (see Cornuault et al. 2018a) and the LM5 epitope in the sodium carbonate and KOH fractions co-elute with this in the unripe tomato samples. In the water extract the epitope elutes earlier indicating a less acidic polymer that is either unlinked to HG or linked to methylesterified HG (see Cornuault et al. 2018a for a discussion of this). Elution profiles for the LM5 epitope are similar in the equivalent fractions of the ripe tomato fruit – albeit at reduced levels. Similar elution profiles are seen for the strawberry fractions – although again at low levels (Fig. 2A). In the case of the LM26 epitope in the same fractions (Fig. 2B), it is scarcely detected in the tomato samples and the unripe strawberry samples but is abundant in the ripe strawberry fractions and shows the same pattern of elution across extracts as does the LM5 epitope.

The LM26 epitope is linked to complex matrix polysaccharides in ripe strawberry cell walls

The specific LM26-branched galactan population detected in ripe strawberry fruit cell wall samples was further evaluated by study of epitope EDC co-elution patterns and sandwich ELISA analyses. Indeed, the full potential of EDC technique is reached when several mAbs are used as detection tools for the same sample. Fig. 3A shows EDC profiles for pectic galactan epitopes (LM5, LM26) along with pectic arabinan (LM6-M, LM13), RG-I backbone (INRA-RU1) and xyloglucan (LM25) epitopes in the sodium carbonate fraction of ripe strawberry cell walls as this is the cell wall fraction with the highest LM26 signal. All epitopes eluted similarly in a peak at 38 ml, co-eluting with the LM19 unesterified HG epitope. Further evidence for linkages between these epitopes was obtained by sandwich-ELISA analyses using CBM77 that binds to unesterified HG (Venditto et al. 2016) as a capture molecule (Fig. 3B). In all cases, signals for epitopes in molecules that bound to CBM77 were higher for strawberry than tomato. The highest signals were obtained for LM19, which has a similar epitope to CBM77, followed by INRA-RU1 and LM6-M. Clear signals for the LM26 and LM5 epitopes were detected for the strawberry cell wall fraction but not tomato. Taken together these observations indicate that the branched galactan epitope in ripe strawberry cell walls is a component of large pectic supramolecules and requires alkali for extraction.

This article is protected by copyright. All rights reserved.

Accepted Article

To explore further the basis for the detection of the LM26 epitope in ripe but not unripe strawberry fruit cell walls, a cellulase treatment of post-KOH cell wall residues was carried out. The rationale for this was to study if ripening-related modulation of the LM26 epitope was related to a set of pectic molecules that was tightly linked with cellulose microfibrils. It was hypothesised that ripening-related changes may result in a reduced detection of galactans in the cellulose fraction and an increased detection of galactans in alkali-soluble fractions. The results of the sequential CDTA, KOH and cellulase extractions of unripe and ripe tomato and strawberry cell walls is shown as an ELISA heat map in Fig. 4. It was notable that significant amounts of both the LM26 and the LM5 epitopes could be released by the cellulase treatment indicating strong association with cellulose microfibrils. However, no evidence was obtained to indicate the abundant presence of the LM26 epitope in cell walls of unripe fruit or that cellulose-microfibril associated galactan was related to the specific abundant detection of the LM26 epitope in ripe strawberry fruit.

The LM26 branched galactan is detected in all cell walls and is abundant in vascular tissues of ripe strawberry fruit

As recently described by Torode et al. 2018, the LM26 branched galactan epitope is specifically detected in phloem sieve elements in several systems. In the case of the strawberry fruit the LM26 epitope was detected in all primary cell walls of ripe fruit albeit at a relatively low level but at an increased level relative to unripe fruit cell walls (Fig. 5). The in situ analyses of ripe strawberry fruit cell walls indicated that the LM26 epitope was abundantly present in a range of parenchyma cell walls associated with both the phloem and also xylem tissues but was notably absent from the cell walls of the phloem sieve elements themselves (Fig. 5).

Discussion

Tomato and strawberry are leading model systems for the study of fruit ripening (Seymour et al. 2013, Wang et al. 2018, Posé et al. 2018). Although much is known about cell wall disassembly during fruit ripening, a full molecular description of events has not yet been achieved (Brummell 2006, Mercado et al. 2011, Wang et al. 2018, Posé et al. 2018). In both fruits, several studies demonstrate a correlation between pectin depolymerisation, loss of neutral sugars from pectin side chains and firmness changes, together with transpirational water loss due to cuticle changes (Saladié et al. 2007). Functional analyses through the downregulation of pectinases (pectate lyase, polygalacturonase and β-galactosidase) have demonstrated direct effects on their respective cell wall targets together with firmer fruit phenotypes in strawberry (Santiago-Doménech et al. 2008, Posé et al. 2013, Paniagua et al. 2016). Contradictory results in the case of tomato have been reported with non-firmer phenotypes for transgenic lines with polygalacturonase (Sheehy et al. 1988, Smith et al. 1988) or β-galactosidase genes downregulated (de Silva and Verhoeyen 1998, Carey et al. 2001, Moctezuma et al. 2003), while

This article is protected by copyright. All rights reserved.

Accepted Article

fruit softening reduction was achieved in the case of downregulation of pectate lyase (Uluisik et al. 2016) and β-galactosidase genes (Smith et al. 2002).

In the current study, we add the detection of the novel LM26 branched galactan epitope in ripe strawberry fruit cell walls to current knowledge of changes to pectic structures during ripening. Our analyses indicate that the LM26 epitope in ripe fruit is a part of RG-I and associated with HG in what may be a large polysaccharide complex in the cell wall matrix. Recent studies are providing evidence against the model of an independent cellulose-hemicellulose network and support the idea that pectins are more intimately linked into cellulose microfibrils than previously appreciated (Wang et al. 2015, Zhang et al. 2016). Our cellulase deconstruction of post-alkali-extracted cellulose residues releasing microfibril-trapped polymers does indicate abundant sets of the pectic galactan epitopes, particularly for the LM5 epitope in both unripe tomato and strawberry cell walls and the LM26 epitope in ripe strawberry cell walls (Fig. 4). As we did not detect high levels of the LM26 epitope in the cellulase-released fraction of unripe strawberry fruit cell walls, the current hypothesis is that the LM26 epitope arises from an altered pectic galactan metabolism during strawberry fruit ripening and is not directly due to ripening-induced changes to cellulose microfibrils. Galactan metabolism could proceed from enzymatic modifications of a complex branched structure exposing the LM26 epitope structure or alternatively de novo synthesis and deposition of the branched structure as an aspect of strawberry ripening. The significance of the branched galactan structure may also relate to modifications that would prevent or influence the degradation of linear 1,4-galactan chains during ripening. The relative increase in galactosyl residues, indicative of branched galactan of RG-I at later developmental stages, has been demonstrated for flax fibers (Mikshina et al. 2012).

The in situ analysis in sections of strawberry fruit confirm the abundance of the LM5 epitope in cell walls of both unripe and ripe fruit and also the relatively increased detection of the LM26 branched galactan epitope throughout the parenchyma cell walls of ripe fruit (Fig. 5A). The LM26 epitope was abundantly detected in sets of parenchyma cells of the vascular tissues of ripe strawberry fruit – but distinct from studies in other systems (Torode et al. 2018) was not detected in the phloem sieve element cell walls (Fig. 5B). The identification and functional significance of these specific sets of vascular cells with the branched galactan epitope is far from clear. Previous studies have demonstrated both phloem sieve element specificity in certain systems and also the widespread distribution of the LM26 epitope in garlic bulb cell walls (Torode et al. 2018). The occurrence of branched galactan has been implicated with a higher elasticity of cell walls (Mikshina et al. 2012, Torode et al. 2018). The vascular tissue of strawberry fruits is under high positive turgor pressures especially during the green-white developmental stage (Pomper and Breen 1997) and an increased cell wall elasticity in particular cells may be required during fruit enlargement. The water requirements of fruit crops, including strawberry, are high (El-Farhan and Pritts 1997). The developmental appearance of the LM26 branched galactan epitope during strawberry fruit ripening may relate to the changing physiology of the fleshy enlarged receptacle, involving both the

This article is protected by copyright. All rights reserved.

Accepted Article

parenchyma primary cell walls and vasculature cell mechanics, in contrast to tomato that directly develops from the ovary of the flower (Giovannoni 2004).

Fruits, being pectin-enriched, offer a source of insoluble fibers and bioactive components for healthy diets and stabilizer and emulsifier polymers for the food industry (Christiaens et al. 2016). The elucidation of the structure-function relationships of pectin has multiple potential applications in both plant biology and food science. Future prospects in this field are promising and recent advances studying cell wall dynamics at the nanoscale and polymer modelling (e.g. Makshakova et al. 2017, Zhang et al. 2016) as well as the advent of novel molecular probes (such as LM26) that enable the tracking of specific structural features, are useful tools in this regard. A more detailed understanding of pectin heterogeneity, dynamics and architectural functions in cell walls has the potential to underpin the future tailoring of pectins to achieve firmer fruit textures and extended shelf lives.

Author contributions

S.P. carried out the work and S.E.M. contributed to the cellulase deconstruction analyses. S.P. and J.P.K. designed the experiments and wrote the manuscript.

Acknowledgements – This research was supported by a Marie Curie Intra European Fellowship to SP within the 7th European Community Framework Programme (PIEF-GA-2013-625270). We thank Martin Fuller (University of Leeds) and Cristina Lucena-Serrano (University of Málaga) for technical assistance in the sectioning of plant materials.

References

Andersen MCF, Boos I, Marcus SE, Kračun SK, Willats WGT, Knox JP, Clausen MH (2016) Characterization of the LM5 pectic galactan epitope with synthetic analogues of β-1,4-D-galactotetraose. Carbohydr Res 436: 36-40

Brummell DA (2006) Cell wall disassembly in ripening fruit. Funct Plant Biol 33: 103-119

Burton RA, Gidley MJ, Fincher GB (2010) Heterogeneity in the chemistry, structure and function of plant cell walls. Nature Chem Biol 6: 724-732

Caffall KH, Mohnen D (2009) The structure, function and biosynthesis of plant cell wall pectic polysaccharides. Carbohydr Res 344: 1879-1900

Carey AT, Smith D, Harrison E, Bird CR, Gross KC, Seymour GB, Tucker GA (2001) Down-regulation of a ripening-related β-Galactosidase gene (TBG1) in transgenic tomato fruits. J Exp Bot 52: 663–668

Christiaens S, Van Buggenhout S, Houben K, Jamsazzadeh Kermani Z, Moelants KRN, Ngouémazong ED, Van Loey A, Hendrickx MEG (2016) Process–structure–function relations of pectin in food. Crit Rev Food Sci Nutr 56: 1021-1042

This article is protected by copyright. All rights reserved.

Accepted Article

Cornuault V, Manfield IW, Ralet MC, Knox JP (2014) Epitope detection chromatography: a method to dissect the structural heterogeneity and inter□connections of plant cell□wall matrix glycans. Plant J 78: 715-722

Cornuault V, Buffetto F, Marcus SE, Crépeau MJ, Guillon F, Ralet MC, Knox JP (2017) LM6-M: a high avidity rat monoclonal antibody to pectic α-1,5-L-arabinan. bioRxiv 161604: doi.org/10.1101/161604

Cornuault V, Posé S, Knox JP (2018a) Disentangling pectic homogalacturonan and rhamnogalacturonan-I polysaccharides: evidence for sub-populations in fruit parenchyma systems. Food Chem 246: 275-285

Cornuault V, Posé S, Knox JP (2018b) Extraction, texture analysis and polysaccharide epitope mapping data of sequential extracts of strawberry, apple, tomato and aubergine fruit parenchyma. Data in Brief 17: 314-320

de Silva J, Verhoeyen ME (1998) Production and characterization of antisense exo-galactanase tomatoes. In: Kuiper HA. eds. Report of the Demonstration Program on Food Safety Evaluation of Genetically Modified Foods as a Basis for Market Introduction. The Netherlands Ministry of Economic Affairs: The Hague, pp 99–106

El-Farhan AH, Pritts MP (1997) Water requirements and water stress in strawberry. Adv Strawberry Res 16: 5-12

Giovannoni JJ (2004) Genetic regulation of fruit development and ripening. Plant Cell 16: S170-S180

Harker FR, Redgwell RJ, Hallett IC, Murray SH (1997) Texture of fresh fruit. Hortic Rev 20: 121–224

Höfte H, Voxeur A (2017) Plant cell walls. Current Biol 27: R865-R870

Jiménez-Bermúdez S, Redondo-Nevado J, Muñoz-Blanco J, Caballero JL, López-Aranda JM, Valpuesta V, Pliego-Alfaro F, Quesada MA, Mercado JA (2002) Manipulation of strawberry fruit softening by antisense expression of a pectate lyase gene. Plant Physiol 128: 751-759

Lee KJD, Dekkers BJW, Steinbrecher T, Walsh CT, Bacic A, Bentsink L, Leubner-Metzger G, Knox JP (2012) Distinct cell wall architectures in seed endosperms in representatives of the Brassicaceae and Solanaceae. Plant Physiol 160: 1551–1566

Makshakova ON, Gorshkova TA, Mikshina PV, Zuev YF, Perez S (2017) Metrics of rhamnogalacturonan I with β-(1→4)-linked galactan side chains and structural basis for self-aggregation. Carbohyr Polym 158: 93-101

Mercado JA, Pliego-Alfaro F, Quesada MA (2011) Fruit shelf life and potential for its genetic improvement. In Jenks, M. A., Bebeli, P.J. (eds.) Breeding for Fruit Quality, pp 81-104. Oxford: John Wiley & Sons.

Mikshina PV, Gurjanov OP, Mukhitova FK, Petrova AA, Shashkov AS, Gorshkova TA (2012) Structural details of pectic galactan from the secondary cell walls of flax (*Linum usitatissimum* L.) phloem fibres. Carbohydr Polym 87: 853-861

This article is protected by copyright. All rights reserved.

Accepted Article

Moctezuma E, Smith DL, Gross KC. (2003) Antisense suppression of a β-galactosidase gene (TBG6) in tomato increases fruit cracking. J Exp Bot 54: 2025–2033

Paniagua C, Blanco-Portales R, Barceló-Muñoz M, García-Gago JA, Waldron KW, Quesada MA, Muñoz-Blanco J, Mercado JA (2016). Antisense down-regulation of the strawberry β-galactosidase gene *FaβGal4* increases cell wall galactose levels and reduces fruit softening. J Exp Bot 67: 619-631

Paniagua C, Santiago-Doménech N, Kirby AR, Gunning AP, Morris VJ, Quesada MA, Matas AJ, Mercado JA (2017) Structural changes in cell wall pectins during strawberry fruit development. Plant Physiol Biochem 118: 55-63

Pedersen HL, Fangel JU, McCleary B, Ruzanski C, Rydahl MG, Ralet M-C, Farkas V, von Schantz L, Marcus SE, Andersen MCF, Field R, Ohlin M, Knox JP, Clausen MH, Willats WGT (2012) Versatile high-resolution oligosaccharide microarrays for plant glycobiology and cell wall research. J Biol Chem 287: 39429-39438

Perkins-Veazie PM, Huber DJ, Brecht JK (1995) Characterization of ethylene production in developing strawberry fruit. Plant Growth Reg 17: 33-39

Pomper KW, Breen PJ (1997) Expansion and osmotic adjustment of strawberry fruit during water stress. J Amer Soc Hortic Sci 122: 183-189

Posé S, Paniagua C, Cifuentes M, Blanco-Portales R, Quesada MA, Mercado JA (2013) Insights into the effects of polygalacturonase FaPG1 gene silencing on pectin matrix disassembly, enhanced tissue integrity, and firmness in ripe strawberry fruits. J Exp Bot 64: 3803-3815

Posé S, Paniagua C, Matas AJ, Gunning AP, Morris VJ, Quesada MA, Mercado JA (2018) A nanostructural view of the cell wall disassembly process during fruit ripening and postharvest storage by atomic force microscopy. Trends Food Sci Technol doi: 10.1016/j.tifs.2018.02.011.

Quesada MA, Blanco-Portales R, Posé S, García-Gago JA, Jiménez-Bermúdez S, Muñoz-Serrano A, Caballero JL, Pliego-Alfaro F, Mercado JA, Muñoz-Blanco J (2009) Antisense down-regulation of the FaPG1 gene reveals an unexpected central role for polygalacturonase in strawberry fruit softening. Plant Physiol 150: 1022-1032

Ralet MC, Tranquet O, Poulain D, Moïse A, Guillon F (2010) Monoclonal antibodies to rhamnogalacturonan I backbone. Planta 231: 1373–1383

Redgwell RJ, MacRae E, Hallett I, Fischer M, Perry J, Harker R (1997a) In vivo and in vitro swelling of cell walls during fruit ripening. Planta 203: 162-173

Redgwell RJ, Fischer M, Kendal E, MacRae EA (1997b) Galactose loss and fruit ripening: high-molecular-weight arabinogalactans in the pectic polysaccharides of fruit cell walls. Planta 203: 174-181

Renard CM (2005) Variability in cell wall preparations: quantification and comparison of common methods. Carbohydr Polym 60: 515-522

This article is protected by copyright. All rights reserved.

Accepted Article

Ruprecht C, Bartetzko MP, Senf D, Dallabernardina P, Boos I, Andersen MCF, Kotake T, Knox JP, Hahn MG, Clausen MH, Pfrengle F (2017) A synthetic glycan microarray enables epitope mapping of plant cell wall glycan-directed antibodies. Plant Physiol 175: 1094-1104

Saladié M, Matas AJ, Isaacson T, Jenks MA, Goodwin SM, Niklas KJ, Xiaolin R, Labavitch JM, Shackel KA, Fernie AR, Lytovchenko A, O'Neill MA, Watkins CB, Lytovchenko A (2007) A reevaluation of the key factors that influence tomato fruit softening and integrity. Plant Physiol 144: 1012-1028

Santiago-Doménech N, Jiménez-Bemudez S, Matas AJ, Rose JKC, Muñoz-Blanco J, Mercado JA, Quesada MA (2008) Antisense inhibition of a pectate lyase gene supports a role for pectin depolymerization in strawberry fruit softening. J Exp Bot 59: 2769-2779

Seymour GB, Colquhoun IJ, Dupont MS, Parsley KR, Selvendran RR (1990) Composition and structural features of cell wall polysaccharides from tomato fruits. Phytochem 29: 725-731

Seymour GB, Østergaard L, Chapman NH, Knapp S, Martin C (2013) Fruit development and ripening. Ann Rev Plant Biol 64: 219-241

Sheehy RE, Kramer MK, Hiatt, WR (1988) Reduction of polygalacturonase activity in tomato fruit by antisense RNA. Proc Natl Acad Sci USA 85: 8805–8809

Smith CJS, Watson CF, Ray J, Bird CR, Morris PC, Schuch W, Grierson D (1988) Antisense RNA inhibition of polygalacturonase gene expression in transgenic tomatoes. Nature 334: 724–726

Smith DL, Abbott JA, Gross KC (2002) Down-regulation of tomato β-galactosidase 4 results in decreased fruit softening. Plant Physiol 129: 1755-1762

Tomato Genome Consortium. (2012) The tomato genome sequence provides insights into fleshy fruit evolution. Nature 485: 635-641

Torode TA, O'Neill R, Marcus SE, Cornuault V, Posé S, Lauder RP, Kračun SK, Rydahl MG, Andersen MCF, Willats WGT, Braybrook SA, Townsend BJ, Clausen MH, Knox JP (2018) Branched pectic galactan in phloem-sieve-element cell walls: implications for cell mechanics. Plant Physiol 176: 1547-1558

Uluisik S, Chapman NH, Smith R, Poole M, Adams G, Gillis RB, Besong TMD, Sheldon J, Stiegelmeyer S, Perez L, Samsulrizal N, Wang D, Fisk ID, Yang N, Baxter C, Rickett D, Fray R, Blanco-Ulate B, Powell ALT, Harding SE, Craigon J, Rose JKC, Fich EA, Sun L, Domozych DS, Fraser PD, Tucker GA, Grierson D, Seymour GB (2016) Genetic improvement of tomato by targeted control of fruit softening. Nature Biotech 34: 950-952

Venditto I, Luis AS, Rydahl M, Schückel J, Fernandes VO, Vidal-Melgosa S, Bule P, Goyal A, Pires VMR, Dourado CG, Ferreira LMA, Coutinho PM, Henrissat B, Knox JP, Baslé A, Najmudin S, Gilbert HG, Willats WGT, Fontes CMGA (2016) Complexity of the *Ruminococcus flavefaciens* cellulosome reflects an expansion in glycan recognition. Proc Natl Acad Sci USA 113: 7136–7141

This article is protected by copyright. All rights reserved.

Accepted Article

Verhertbruggen Y, Marcus SE, Haeger A, Verhoef R, Schols HA, McCleary BV, McKee L, Gilbert HJ, Knox JP (2009a) Developmental complexity of arabinan polysaccharides and their processing in plant cell walls. Plant J 59: 413-425

Verhertbruggen Y, Marcus SE, Haeger A, Ordaz-Ortiz JJ, Knox JP (2009b) An extended set of monoclonal antibodies to pectic homogalacturonan. Carbohydr Res 344: 1858–1862

Wang T, Park YB, Cosgrove DJ, Hong M (2015) Cellulose-pectin spatial contacts are inherent to never-dried Arabidopsis thaliana primary cell walls: evidence from solid-state NMR. Plant Physiol 168: 871-884

Wang D, Yeats TH, Uluisik S, Rose JKC, Seymour GB (2018) Fruit softening: revisiting the role of pectin. Trends Plant Sci 23:302-310

Zhang T, Zheng YZ, Cosgrove DJ (2016) Spatial organization of cellulose microfibrils and matrix polysaccharides in primary plant cell walls as imaged by multichannel atomic force microscopy. Plant J 85: 179-192

Figure legends

Fig. 1. Glycomic heat-maps of the main pectic epitopes detected in solubilized fractions of tomato and strawberry fruits at unripe and ripe stages. Sequential extracts of cell wall residues of each sample were made with reagents of increasing stringency (phenol, water, CDTA, Na_2CO_3 and KOH). Cell wall extracts (60-fold dilutions) were loaded onto ELISA plates and screened against an array of pectic-directed mAbs (right hand side column). Values shown are the % of the maximal detectable signal from across the ELISAs and are means of biological triplicates. White signifies no binding and darker green representing the strongest binding/epitope detection.

Fig. 2. Epitope detection chromatography (EDC) profiles of galactan epitopes in extracts of tomato and strawberry fruit at unripe and ripe stages. LM5 (A) and LM26 (B). EDC profiles of CWM solubilized by water (light-orange), sodium carbonate (black dotted) and KOH (dark-blue). AEC salt gradient from 0 to 0.3 M and from 0.3 to 0.6 M of NaCl is shown as a grey dotted line. Vertical dotted lines indicate elution position of unesterified pectic HG epitopes. Profiles shown are at least duplicate means.

Fig. 3. (A) Epitope detection chromatography (EDC) profiles of sodium carbonate-soluble fraction of strawberry-ripe cell walls showing co-elution of the LM26 epitope with the LM5, INRA-RU1, LM6-M, LM13 and LM25 xyloglucan epitope. HG elution is indicated by the vertical black dotted line.

This article is protected by copyright. All rights reserved.

Accepted Article

AEC salt gradient with NaCl (0 to 0.3 M and from 0.3 to 0.6 M) is shown by the grey dotted line. Averaged profiles from at least two biological replicates. (B) Sandwich-ELISA using HG-binding CBM77 as capture probe for cell wall polysaccharides and the same set of pectin and xyloglucan mAbs as detection probes after incubation with sodium carbonate fraction of ripe strawberry and tomato fruit.

Fig. 4. Heat map of the presence of the LM26 and LM5 pectic galactan epitopes in extracts of unripe (UR) and ripe (R) of tomato and strawberry fruit. CWMs were sequentially extracted with CDTA, KOH and cellulase and solubilized materials titrated on microtitre plates. ELISA absorbance values shown are for 1250-fold dilutions of the extracts for LM26 and 6250-fold dilutions for LM5. Values are means of technical triplicates. Relative intensity shading is applied separately for the two mAbs.

Fig. 5. Indirect immunofluorescence labelling of pectic galactan epitopes, on resin sections of strawberry fruits at unripe and ripe stages. (A) Micrographs of parenchyma tissues: LM26, LM5 and negative controls without primary mAb (No mAb). (B) Micrographs of a vascular bundle shown in bright field (Vb - BF), the same region with Toluidine Blue O staining (Vb - TBO) and detection of the LM26 epitope (Vb – LM26) as well as merged image of TBO staining and LM26 immunofluorescence. Ph, phloem; Xy, xylem; arrowheads indicate sieve plates; asterisks indicate lignified xylem vessels. Scale bars A: 100 µm; B: 20 µm.

This article is protected by copyright. All rights reserved.

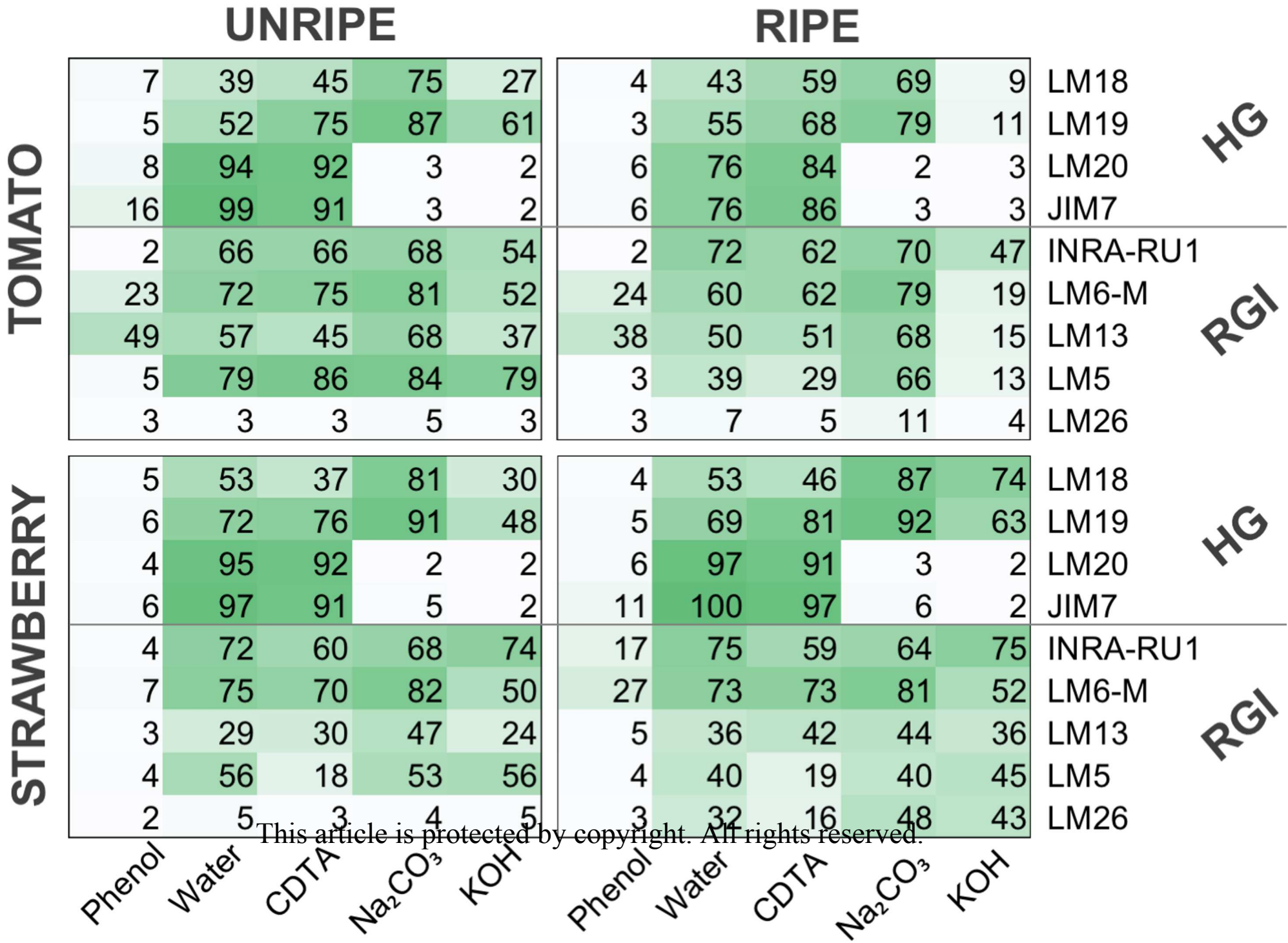

This article is protected by copyright. All rights reserved.

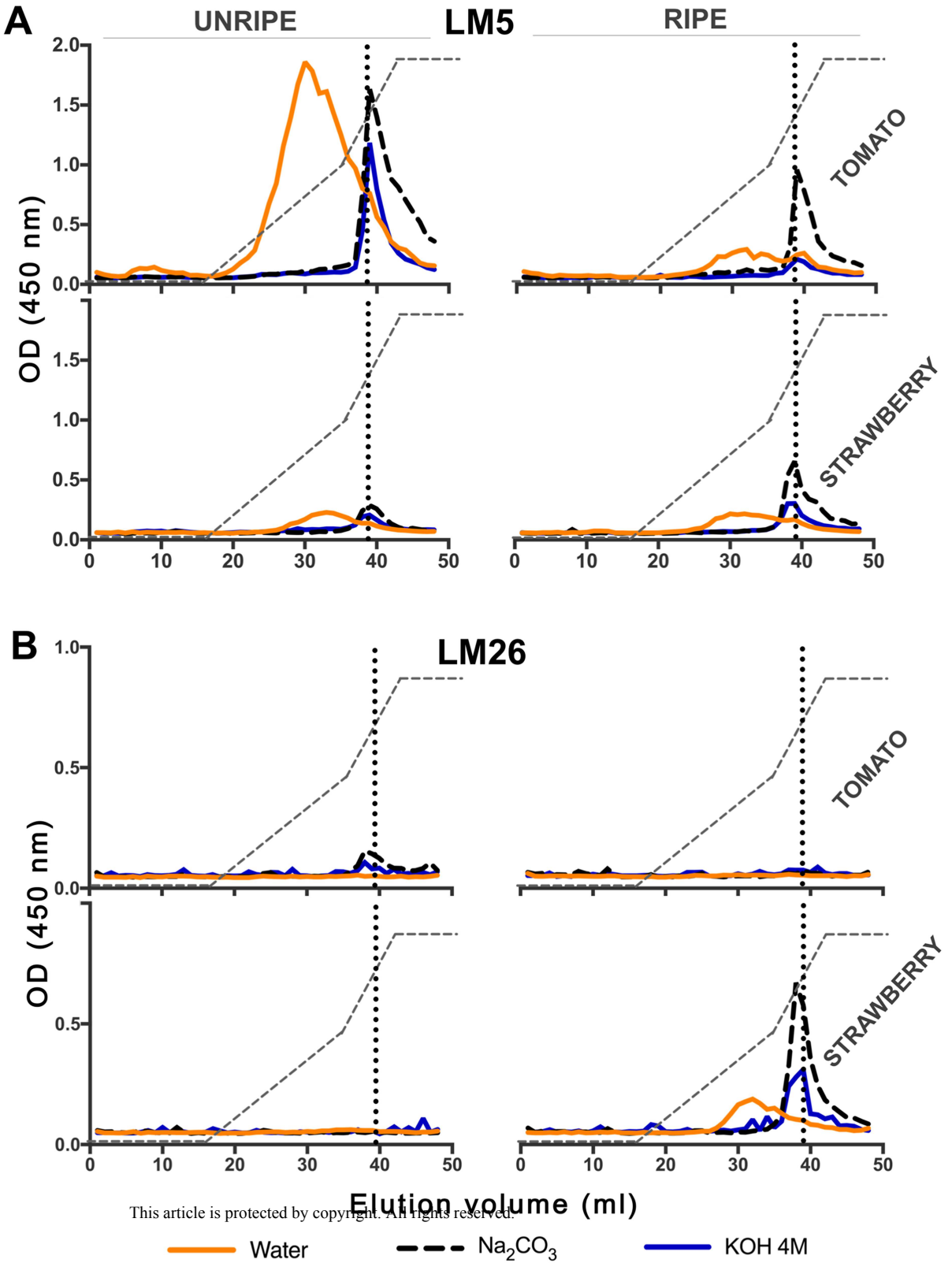

This article is protected by copyright. All rights reserved.

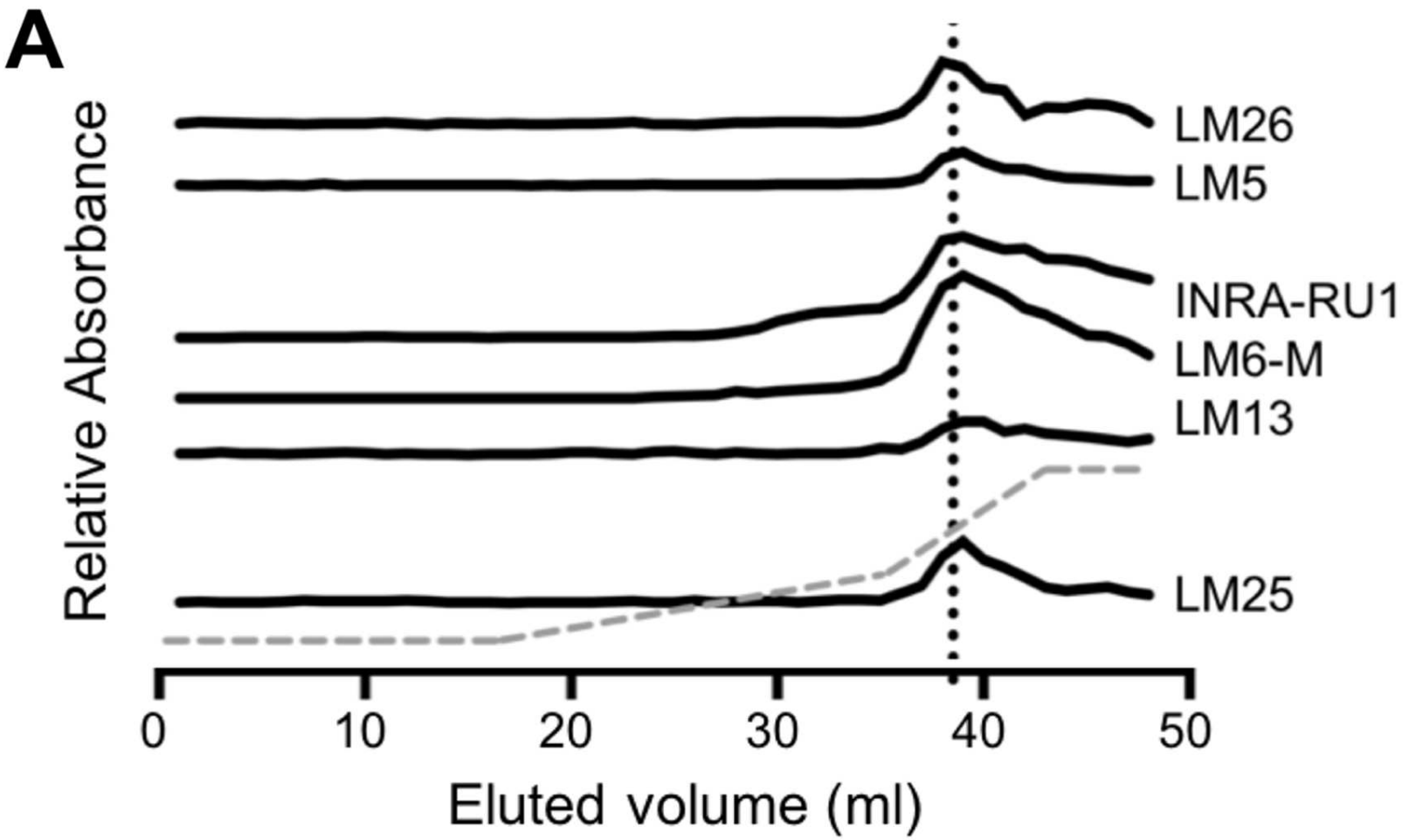

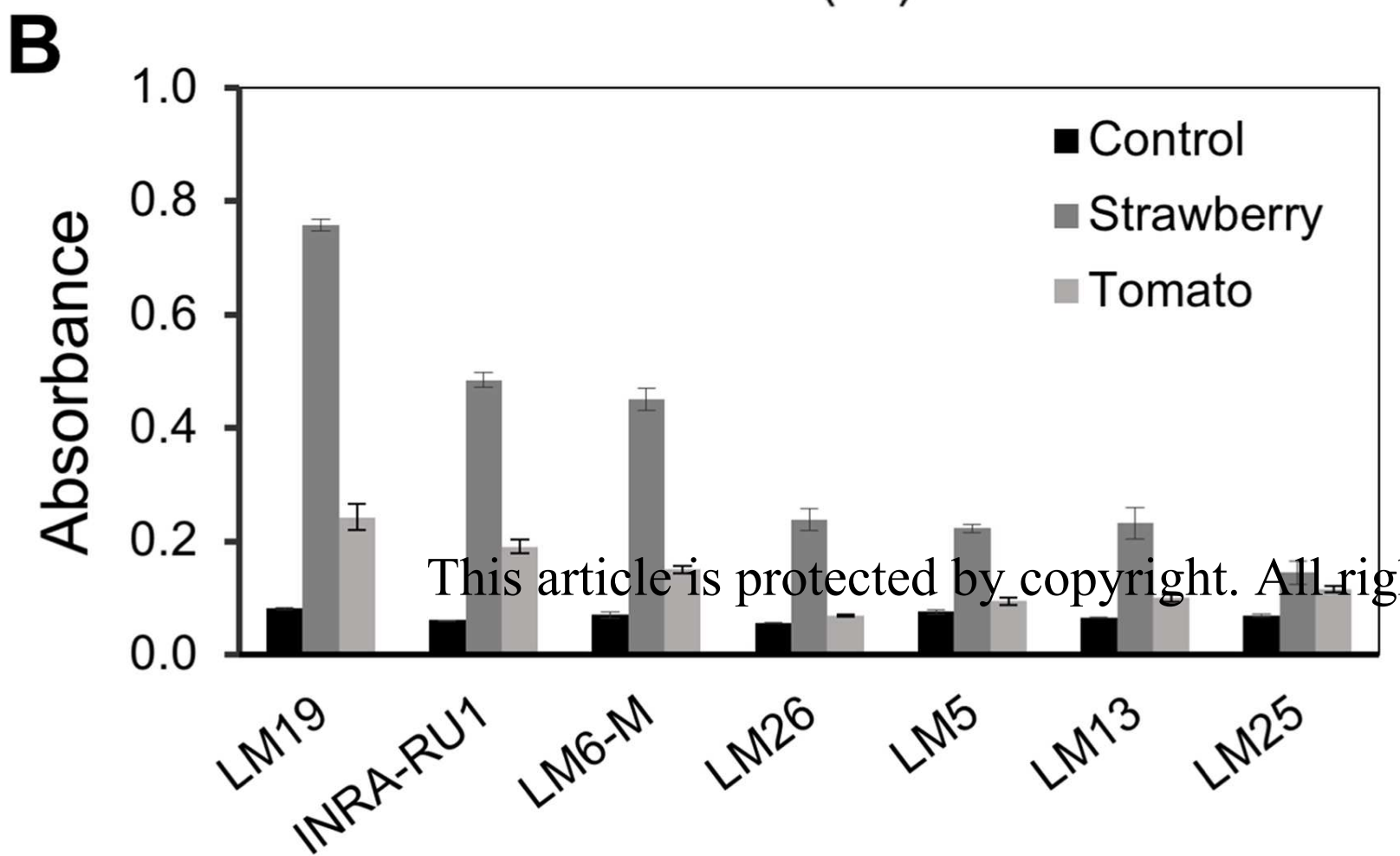

This article is protected by copyright. All rights

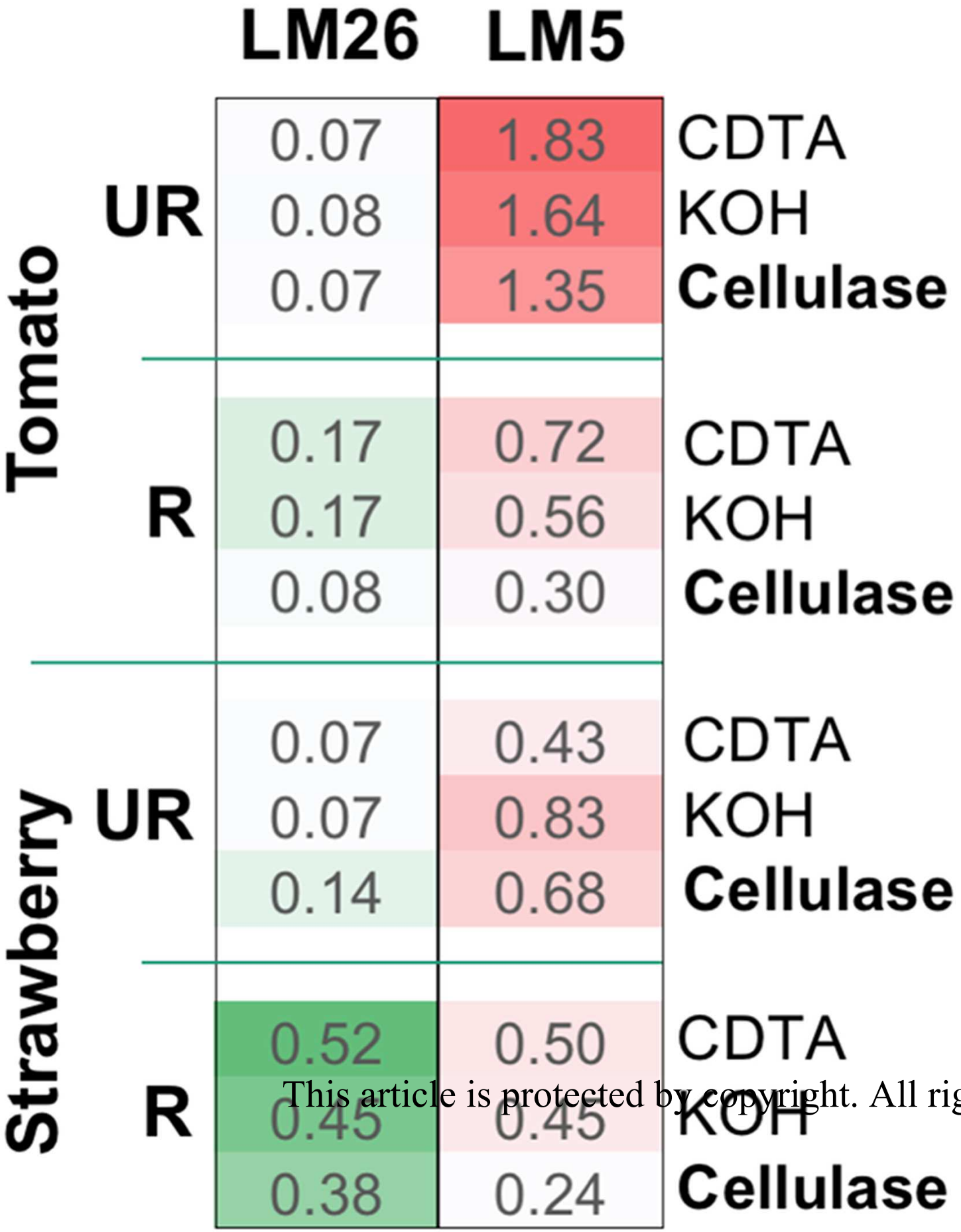

This article is protected by copyright. All rights

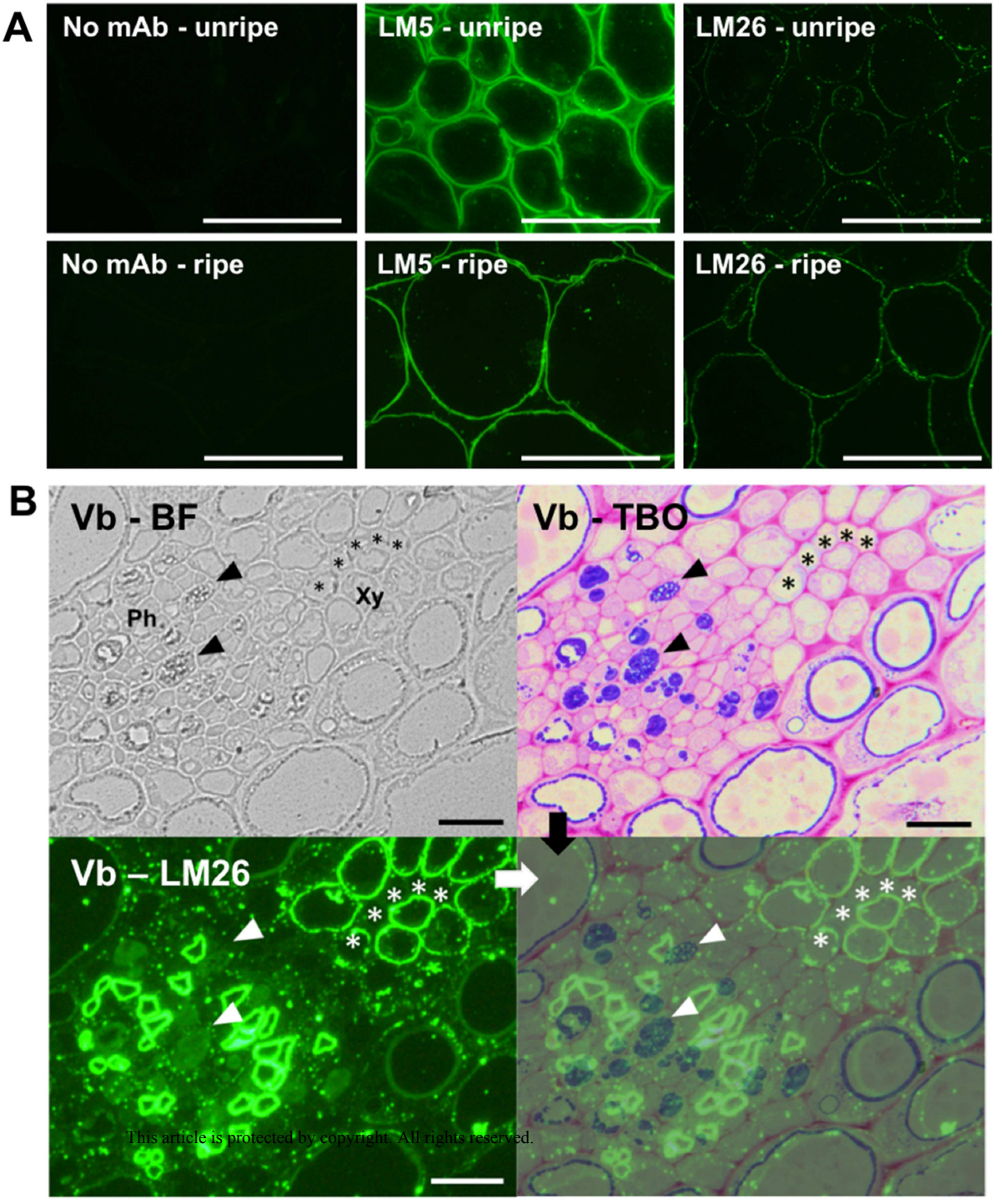

This article is protected by copyright. All rights reserved.